J. Fluid Mech. (1983), *vol.* 127, *pp.* 27–44
Printed in Great Britain

The effects of stable stratification on turbulent diffusion and the decay of grid turbulence

By R. E. BRITTER,
Department of Engineering, University of Cambridge, Cambridge CB2 1PZ

J. C. R. HUNT,†
Department of Applied Mathematics and Theoretical Physics, University of Cambridge, Cambridge CB3 9EW

G. L. MARSH
Northrop Services, Inc., Research Triangle Park, North Carolina 27709

AND W. H. SNYDER‡
Meteorology and Assessment Division, Environmental Sciences Research Laboratory, U.S. Environmental Protection Agency, Research Triangle Park, North Carolina 27711

(Received 3 June 1981 and in revised form 8 September 1982)

Experiments are described in which a grid is towed horizontally along a large tank filled first with water and then with a stably stratified saline solution. The decay rates of the r.m.s. turbulent velocity components (w', v') perpendicular to the mean motion are measured by a 'Taylor' diffusion probe and are found to be unaffected by the stable stratification over distances measured from 5 to 47 mesh lengths (M) downstream, and over a range of Froude number U/NM of ∞ and 8·5 to 0·5, U being the velocity and N the buoyancy frequency. The Reynolds number Mw'/ν of the turbulence was about 10^3, where ν is the kinematic viscosity. The vertical velocity fluctuations produced near the grid were reduced by the stratification by up to 30 % when $U/MN \approx 0{\cdot}5$. Large-scale internal wave motion was not evident from the observations within about 50 mesh lengths of the grid.

The turbulent diffusion from a point source located 4·7 mesh lengths downstream was studied. σ_y, σ_z, the horizontal and vertical plume widths, were measured by a rake of probes. σ_y was found to be largely unaffected by the stratification and grew like $t^{\frac{1}{2}}$, while σ_z was found in all cases to reach an asymptotic limit $\sigma_{z\infty}$ where $0{\cdot}5 \leqslant \sigma_{z\infty} N/w'_s \leqslant 2$, w'_s being the r.m.s. velocity fluctuations at the source; the time taken for σ_z to reach its maximum was about $2N^{-1}$. These results are largely in agreement with the theoretical models of Csanady (1964) and Pearson, Puttock & Hunt (1983).

1. Introduction

1.1. *Experimental objectives and implications*

The laboratory experiments reported here were designed to answer two questions about the effects of stable stratification on the rate of homogeneous decay of turbulence and on turbulent diffusion from a point source in the decaying turbulence.

† Also Department of Engineering.

‡ On assignment from the National Oceanic and Atmospheric Administration, United States Department of Commerce.

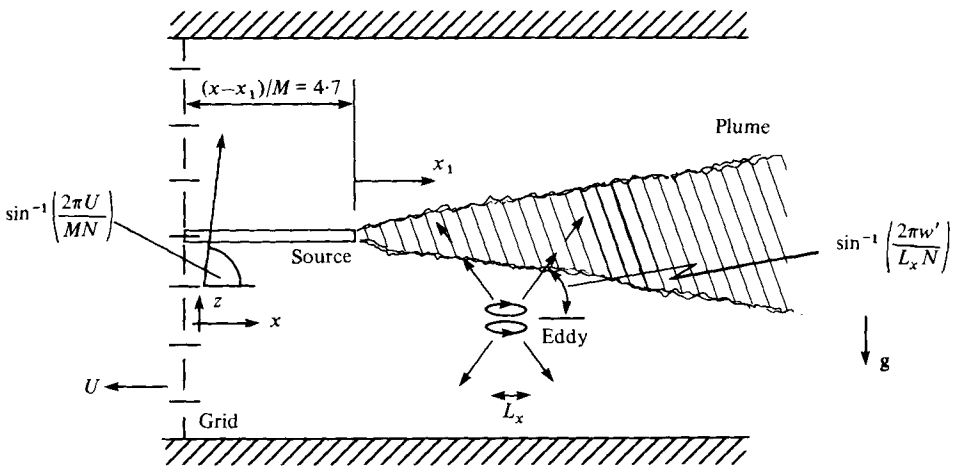

FIGURE 1. Schematic diagram of experiment.

(i) How does the stratification affect the turbulence produced near a grid and beyond what distance downstream of a grid is the decay of turbulence appreciably affected by the stratification?

(ii) Does the stratification not merely reduce but change qualitatively the vertical diffusion of marked particles (e.g. a stream of dye)? Different theories and interpretations disagree as to whether the depth of such plumes must always continue to grow parabolically, albeit at a reduced rate, or whether they must effectively cease growing even while the velocity fluctuations persist.

In §1.2 we discuss the physical processes of decay and diffusion to explain the significance of these questions and the value of the experiments. Although the processes of decay and diffusion are rather subtle, the advantages of better understanding of stratified turbulent flows are clear, especially to help predict the dispersion of pollutants in the atmosphere and in coastal or river waters. Our experiments were restricted to decaying turbulence. However, it is interesting to note that there are a number of environmental flows where the turbulence is also decaying in stable density gradients, for example in the wakes of towed object (Pao 1971), in the stable atmosphere in the lee of buildings or hills, on the continental shelf (Armi 1978), and in the atmospheric or oceanic surface layers where stable stratification is suddenly imposed.

1.2. *Some theoretical ideas about decay and diffusion in stable density gradients*

1.2.1. *Decay.* Consider a grid (see figure 1) with a mesh size M placed in a uniform stable stratification $\partial\bar{\rho}/\partial z$ of a buoyancy frequency

$$N = \left[g\frac{-\partial\bar{\rho}/\partial z}{\bar{\rho}}\right]^{\frac{1}{2}},$$

where the flow through the grid has a velocity U. If the Froude number U/NM is much greater than unity, the inertial forces are much greater than the gravitational forces *near the grid*. But sufficiently far downstream (or sufficiently long after the grid has passed), the r.m.s. vertical turbulent velocity w' decays to a value such that the local Froude number w'/NL_x, based on w' and an integral scale L_x of turbulence for w, becomes much less than unity and the buoyancy forces dominate.

There are three main ways in which these buoyancy forces can affect the rate of decay of turbulent kinetic energy, defined over a volume V as $\dot{T}_V$, where

$$\dot{T}_V = \frac{\partial T_V}{\partial t} = \int_V \left(\tfrac{1}{2}\bar{\rho}\frac{\partial \overline{q^2}}{\partial t}\right) dV. \tag{1}$$

(i) A vertical density flux $\overline{w\rho}$, caused by the turbulence tending to mix elements of fluids of high and low density, also increases the potential energy of fluid elements at a rate $B_V = \int g\,\overline{w\rho}\,dV$. In stationary stratified turbulence this density flux is produced by molecular mixing between the fluid elements and $B_V > 0$ when $d\bar{\rho}/dz < 0$. But in *decaying* turbulence the initial potential energy associated with the vertical displacements Z of the fluid elements from their equilibrium position decays as the turbulence decays. This induces a net negative density flux. In the absence of molecular mixing

$$B_V = \int g\frac{d\overline{Z^2}}{dt}\left(-\frac{d\bar{\rho}}{dz}\right) dV,$$

so $B_V < 0$ when $d\overline{Z^2}/dt < 0$ and $d\bar{\rho}/dz < 0$ (see Pearson, Puttock & Hunt 1983, §4).

(ii) If the volume V has a surface S, the kinetic energy within S can decrease owing to the propagation of internal waves out of S and due to the work done on the fluid outside S. Both effects are represented by $P_V = \int_S \overline{p\mathbf{u}.\mathbf{n}}\,dS$.

(iii) The dissipation of turbulent kinetic energy per unit volume $\rho\epsilon$ can be affected by the stratification, because of its effects on velocity gradients in the turbulence. Thus

$$-\dot{T}_V = B_V + P_V + \int \rho\epsilon\,dV. \tag{2}$$

To what extent do each of these terms affect $\dot{T}_V$ in a grid-turbulence experiment?

(*a*) *Buoyancy flux.* When a grid is towed through a stably stratified fluid, the wakes of the bars (scale b) produce velocity fluctuations with kinetic energy and fluctuating vertical displacements with potential energy ($\sim \rho N^2 b^2$ per unit volume). However the vertical displacements are greater for a horizontal grid moved vertically than for a vertical grid moved horizontally (Linden 1980, figure 1*c*).

In the horizontally towed grid experiments described here we have concentrated on cases where $5 \gtrsim U/NM \gtrsim 0{\cdot}5$ and examined the flow over a range of values of the distance x downstream of the grid such that $0{\cdot}5 > w'/NL_x > 0{\cdot}02$ (taking $L_x \approx \frac{1}{2}M$). Even over this range of stratification we estimate that the direct effect of $\dot{T}_V$ produced by the buoyancy flux B_V is small, based on the observations of the rate of decay of $\overline{Z^2}$ and on the measurement of the net density flux produced by molecular mixing over the period from the grid's passage to the final decay (Britter & Marsh 1982).

(*b*) *Internal-wave energy transfer.* In grid-turbulence experiments in unstratified fluid the streamwise transfer of energy, i.e. $\partial(\overline{up}/\rho + \overline{uq^2})/\partial x$ is small compared with the decay of the turbulence, i.e. $(\overline{q^2})^{\frac{3}{2}}/L_x$, and is usually neglected.

In stably stratified flows, internal gravity waves with frequency ω propagate from a source at an angle to the horizontal of $\theta = \pm\sin^{-1}(\omega/N)$. There are no waves when $\omega > N$. Thus for a turbulent flow with characteristic frequency $\omega \sim 2\pi w'/L_x$, we expect the energy propagation to be greatest in the directions $\theta \sim \pm\sin^{-1}(2\pi w'/L_x N)$. The experiments of McLaren *et al.* (1973) showed how a local source of turbulence (a rising blob of buoyant fluid in their case) propagates energy away on a timescale of N^{-1}. Their experiments also showed that the amplitude of vertical motions near a local source of decaying turbulence is greatest in the *vertical* direction and decreases as θ decreases.

In order for there to be a significant net energy transfer by wave motion in the streamwise direction the gradient of wave energy $\nabla(\overline{\tilde{q}^2})$ and the group velocity $\mathbf{C}_g$ must be large enough so that their product is comparable with the dissipation rate $-d\overline{q^2}/dt$. The ratio of these two terms may be estimated as $\sim \mathbf{C}_g \cdot \mathbf{U}/U^2 \lesssim NL_x/2\pi U$. For most grid-turbulence experiments this estimate shows that P_V is negligible.

However, over a limited period, when $2\pi w'/NL_x \sim 1$ and wave energy grows rapidly, gradients of wave energy and therefore P_V may be larger than given by the above estimate.

In addition to waves generated by the turbulence, internal waves must be generated by the grids themselves, and these may excite the natural internal wave modes of the tank. In a vertical tank, Dickey & Mellor (1980) showed that a grid can excite a mode with frequency N; then velocity measurements have to be separated into their internal mode and turbulence components. In a long horizontal tank, the natural modes are of very low frequency and are negligible in strength compared with the turbulence.

(*c*) *Viscous dissipation.* This discussion of the wave motion is necessary to justify the assumption that, provided $w'/L_xN \gtrsim 0{\cdot}15$, for a horizontally towed grid the turbulent decay is primarily due to local *viscous* processes, i.e. $-\dot{T}_V \approx \int \rho\epsilon\, dV$. How does the stratification affect ϵ? The largest scales of motion (on a scale $\sim w'/N$), are affected even by weak stratification (Dougherty 1961). But on the basis of measurements in the atmospheric boundary layer (e.g. Kaimal 1973), even when $w'/NL_x \sim 1$, the energy cascade processes in the inertial and dissipative sub-ranges of the equilibrium spectra have the same form as in neutrally stratified turbulence. Consequently, by the usual dimensional arguments ϵ should be proportional to w'^3/L_x, where the proportionality factor may be a weak function of w'/NL_x.

In fact, Kaimal's (1973) data show that, in the stable atmosphere boundary layer, $\epsilon L_x/w'^3$ was insensitive to stratification (although L_x, the scale of the vertical component, was itself changed quite markedly at a given distance above the surface). Similarly, in the grid experiment of Dickey & Mellor (1980), $\epsilon L_x/w'^3$ was unaffected for 250 mesh timescales (M/U) after the passage of the grid. Thereafter, strong internal waves dominated the velocity field and ϵ/w'^3 suddenly decreased to nearly zero.

There are some instructive comparisons to be made between the effects of stratification and the effects of rotation on the decay of turbulence. Ibbetson & Tritton (1975) found experimentally that the decay rate was increased by rotation (with initial turbulence Rossby numbers ranging from 28 to 0·3). They reasoned that this was caused by the absorption of inertial wave energy at the boundaries. So one should note that, wherever waves are produced by turbulence, the transmission of energy between regions of different kinetic energy and the reflection, and absorption at boundaries have to be carefully considered in any theoretical or experimental investigation of decaying turbulence.

1.2.2. *Diffusion.* The vertical diffusion of pollutants in turbulence with stable stratification is a subject of controversy. There are apparently two main schools of thought about what happens as the stratification increases. One is that, far from the source, growth of the plume's width σ_z is always effectively described by a diffusivity K_z, so that

$$U\frac{d\sigma_z^2}{dx} = \frac{d\sigma_z^2}{dt} = 2K_z, \tag{3}$$

where K_z is a decreasing function of, say, w'/L_xN. In some models it is suggested that, when $w'/L_xN \ll 1$, K_z should be scaled on N and the viscous dissipation ϵ, so that

$K_z \sim \epsilon N^{-2}$ (Weinstock 1978). The essential basis of such models is Taylor's (1921) analysis of the random motion of a marked particle, which leads to $K_z = w'^2 T_L^{(w)}$, and the assumption that there must be a small but finite Lagrangian integral timescale of the vertical motion $T_L^{(w)}$.

However, Csanady (1964) and recently Pearson *et al.* (1983) have suggested that in stable conditions, where $w'/L_x N \sim 1$, fluid elements cannot move through large vertical distances ($\gtrsim w'/N$) without changing their density, because these elements only have kinetic energy of the order of $\frac{1}{2}\bar{\rho}(w')^2$. Consequently most elements in a plume of marked particles remain within a vertical distance of the order of w'/N of their origin until very slowly (on a timescale long compared with the turbulence decay time) they change their density. For this reason a small density flux can co-exist with a marked limitation of the growth of plumes. Some details of the theory have been published already by Pearson & Britter (1980).

Evidently these two theoretical concepts lead to different predictions for plume behaviour, which we examine in these experiments.

2. Apparatus, instrumentation and experimental procedure

The experiments were conducted in a towing tank 1·2 m deep, 2·4 m wide, and 25 m long. The tank has an aluminium framework, and the sides and bottom are constructed with acrylic plastic for viewing purposes. Rails located on top of the sidewalls provide a support and track for the towing carriage. Models are attached to the carriage and can be towed the length of the tank at speeds in the range 5–50 cm/s.

A salt-water filling system (see Hunt & Snyder 1980) enables various stable density profiles to be established in the tank. The density profiles are determined by drawing water samples from various depths and measuring the specific gravity of the samples with a Mettler (PL200) electronic balance. The specific gravity is measured by placing a weight, suspended from the electronic balance, into each water sample. Initially the weight is placed in a sample of fresh water and the output of the electronic balance is recorded. The specific gravity of each sample is then deduced from the ratio of the output for the sample and the output for fresh water. The absolute error in specific gravity was estimated to be less than 0·0001.

A square-mesh biplanar grid was constructed from rectangular aluminium bars 1·9 cm wide and 1·3 cm thick with a mesh length $M = 8{\cdot}56$ cm. Its solidity was thus 40 %. The grid was rigidly attached to the towing carriage and towed the length of the tank. A neutrally buoyant dye mixture was emitted through a tube downstream of the grid.

The source tube for the dye released was located at the centre of the grid in the lateral direction and approximately 55 cm below the water surface (depending on slight variations in the level of the water surface). The source was directly behind a lateral bar and midway between two vertical bars. The outside and inside diameters of the source tube were 0·64 cm and 0·56 cm respectively, and the tube extended downstream from the rear of the grid 40 cm or 4·71 mesh lengths. The source size was small enough ($< \frac{1}{10}M$) to expect that the mean plume widths would be the same as that defined by the motion of single fluid elements for distances from the source greater than M. The effluent flow rate was adjusted to maintain an isokinetic release based on the outside diameter of the source tube. Blue food dye (Warner–Jenkinson no. 393) was used as the material for flow visualization as well as the quantitative concentration measurements. The dye was diluted by mixing it with water drawn at the level of the source tube in the towing tank. Additional small amounts of

saturated salt water or alcohol were added to obtain a neutrally buoyant effluent. The source mixture was pumped through the tube using a positive displacement pump from a large graduated cylinder. A damper downstream of the pump, in addition to flexible tubing, minimized pulsations in the flow from the tube. The flow rates were preset and also double-checked during each test by measuring initial and final volumes in a graduated cylinder as well as the elapsed time during pumping.

The concentration measurements were obtained by drawing water samples through ports in a rake positioned downstream of the source tube exit. The rake was in the shape of a cross with arms extending in horizontal and vertical directions. The spacing between ports in the lateral direction was 2 cm, while that in the vertical direction was 0·5 cm for ports located from the centre of the rake to 9 cm above and below the centre. For ports located further than 9 cm from the centre, the port spacing was increased to 1 cm.

The ports in the sampling rake were constructed from 0·24 cm outside diameter brass tubing and were connected to a series of boxes by Tygon tubing. During each experiment the grid was towed approximately 11 m while a sample was being drawn through the ports and into corresponding test tubes. Over the towing distance, approximately 50 cc of sample were drawn into each test tube. The dye concentrations contained in these samples were measured with a Brinkman (model PC-600) Probe Colorimeter. It was initially calibrated with a set of 11 dye standards prepared by mixing dye with water drawn from the towing tank at the level of the source tube. These samples ranged in concentration from 0·5 to 0·0001 % in logarithmic steps. The voltage output of the colorimeter was digitized and then averaged on a PDP 11/40 minicomputer. A numerical scheme was used to calculate the 'best-fit' curve to the set of dye-concentration samples. This equation was then used to obtain the concentrations of unknown samples. The wavelength used on the colorimeter was 570 nm.

A density profile was obtained each day before running an experiment. Passage of the grid through the tank would leave the central portion of the density profile linear but result in a nearly neutral stratification at the top and bottom of the tank. Experiments were only conducted when a central region of at least 60 cm in vertical extent had the required linear density profile. For the linear density profiles the buoyancy frequency was $N = 0, 0{\cdot}43, 0{\cdot}96$ and $1{\cdot}33$ rad/s for the neutral and the three stable density stratifications. Although in a linear density profile the buoyancy frequency is not exactly constant, this was an adequate approximation over the central portion of the tank in which diffusion was being studied.

Three tow speeds, $U = 6$, 12 and 30 cm/s, were used, and the plume characteristics measured at $x_1 = 30$, 100, 200, 300 and 415 cm downstream of the source exit. The coordinate x_1 is measured downstream from the source, while the coordinate x is taken from the grid.

For each measured concentration distribution, the centroid ($\bar{y}$ or $\bar{z}$), the standard deviation (σ_y or σ_z) about the centroid and the non-dimensional third and fourth moments were calculated. A least-squares-fit Gaussian curve with the same standard deviation as the measured distribution was also computed.

In order to check on the accuracy of the concentration measurements, the volume flux of dye across the plane where the profiles were taken was compared with the effluent flow rate. Assuming the concentration profiles to be Gaussian, the term

$$G = \frac{2\pi\sigma_y\sigma_z C_{\max g}}{Q}$$

should be unity. $C_{\max g}$ is the maximum concentration in either the vertical or lateral Gaussian profile. In practice, the quantity G deviates from unity because of the inaccuracies of obtaining exact values of the effluent rate, the towing speed, σ_y and σ_z, and the maximum non-dimensional Gaussian concentration. Of course, if the profile shape is not Gaussian, G also differs from unity. However, the profile shapes were nearly Gaussian for all experiments except those when $N = 1{\cdot}33$ rad/s, $U = 6$ cm/s, in which fourth moments much larger than 3 were measured.

It was initially intended to accept only data for which $0{\cdot}75 < G < 1{\cdot}25$, and this criterion led to the rejection of only a small amount of data for $N = 0$, 0·43 and 0·96 rad/s. For the strongest stable density stratification ($N = 1{\cdot}33$ rad/s), the same criterion required that about half the data be discarded. By extending the criterion for $N = 1{\cdot}33$ rad/s to $0{\cdot}75 < G < 1{\cdot}75$, most of the data was acceptable. By way of explanation, it should be noted that the data with $N = 1{\cdot}33$ rad/s were the first data taken with a stable density stratification. Subsequent data were taken with an improved technique for bleaching the dye from the tank after each run and a more frequently repeated calibration of the colorimeter. Inspection of the discarded data suggested that the standard deviations σ_y and σ_z were being correctly measured, but the magnitude of the grouping $C_{\max g}\, U/Q$ was in error.

The concentration profiles were edited by deleting any profiles in which the maximum to minimum concentration ratio on either side of the maximum concentration was less than 5. Using this criterion, more than 95 % of the area under the dye concentration profiles was assured. Also, only profiles in which $|\bar{y}$ (or $\bar{z})| \leqslant 0{\cdot}32\sigma_y$ (or σ_z) were accepted. This ensured that there was no more than a 5 % error in the estimated maximum concentration as a result of misalignment between the plume axis and the sampling rake.

Limited measurements of the velocity fluctuations (not necessarily turbulent velocity fluctuations) were also made downstream of the grid. Some preliminary measurements were made in a homogeneous fluid with a TSI endflow X-film probe (type 124 NACL) driven by a TSI 1053B anemometer. The signals were linearized before being recorded on magnetic tape for subsequent analysis. The probe was calibrated in the towing tank upstream of the grid. Data were digitized at 200 Hz for a period of 20 s. Unfortunately, carriage vibration and probe contamination resulted in low repeatability and poor accuracy. But three experimental runs, two at tow speeds of 30 cm/s and one at 6 cm/s, are presented in §3. Considerable difficulty was experienced in operating the hot-film probes in the stratified fluid and the technique was abandoned until further time was available for investigation of this problem.

An alternative technique for measuring velocity fluctuations was devised by utilizing the statistical theory of diffusion from a continuous source (Taylor 1921). For short diffusion times, i.e. much less than the Lagrangian integral timescale T_{L}, the standard deviation of the lateral or vertical plume spread (σ_y or σ_z) is linearly related to the corresponding standard deviations of the velocity fluctuations (v' or w'). Thus $\sigma_y = v't = v'(s/U)$ and $\sigma_z = w't = w'(s/U)$ for $t = s/U \ll T_{\mathrm{L}}$, where s is the longitudinal distance from the source. The Lagrangian integral scale in the non-stratified grid turbulence may be estimated from diffusion results in §3 as $T_{\mathrm{L}} = 0{\cdot}0128UM/(w')^2$. At the measurement positions closest to the grid ($x/M = 4{\cdot}71$) $t/T_{\mathrm{L}} = s/[0{\cdot}0128M(w'/U)^{-2}]$ was about unity, giving an error of 10 % (Pasquill 1974, p. 132). At all other points t/T_{L} was less than 0·3 with errors of less than 3 %.

When the fluid is stratified, no estimates exist for the Lagrangian integral timescale, although we intend to show later that it becomes very small. The

requirement for the probe is that over the time t the autocorrelation of the particle velocity be near unity. In a stratified turbulent flow this timescale is N^{-1}, so the requirement is that $t < 1/N$ or $s < U/N$. This condition was met in all the experiments.

A miniature source-and-rake arrangement, which we refer to as a 'Taylor' probe, was constructed with a source tube of 0·16 cm outside and 0·08 cm inside diameter. The sampling rake was of similar tubing with spacing between the port centres of 0·25 cm. The sampling ports extended 2·5 cm in all four directions from the centre port. Normally the sampling rake was positioned 10 cm downstream of the source-tube exit. For measurements obtained with the source-tube exit located 40 cm downstream of the grid, the sampling rake was positioned 6 cm downstream of the source-tube exit. When the source-tube exit was located 400 cm downstream of the grid, the separation distance was either 10 or 20 cm. Only slight differences in the plume statistics were seen using these two separation distances. These distances ensured that $s < UT_L$ or $2\pi U/N$ and that an adequate spread in the plume existed at the sampling rake, enabling accurate measurements to be made of the plume statistics and implied velocity fluctuations. This technique was compared with the hot-film data for the homogeneous fluids and gave consistent results. Although we were unable to experimentally validate this technique in the density-stratified fluid, there is sound theoretical justification (Pearson *et al.* 1983).

3. Experimental results

The experimental results are presented in three parts: a qualitative description of the experimental observations (§3.1); a quantitative description of the plume development (§3.2); and velocity measurements taken to elucidate the turbulent structure, and hence the plume behaviour (§3.3).

3.1. *Visual observations*

Acceleration of the grid up to the required velocity produced a very small and decaying surface wave pattern. Apart from this initial disturbance the free surface remained flat for the duration of each experiment except for a slight draw-down and subsequent rise in the immediate lee of the grid. No motion was observed upstream of the grid over the range of variables studied; a not-surprising result given that the minimum value of the relevant non-dimensional parameter U/Nb was 2·37, where b is the bar width. This is considerably larger than $\frac{1}{2}\pi$, the maximum value required for upstream influence (see Turner 1973). No large-scale internal wave motions were obvious for $x/M < 50$, however at $x/M \gg 50$ internal waves were observed with little turbulence and these were maintained to a considerable distance (or time).

When U/NM was small a set of two-dimensional jets was formed throughout the depth of the tank *well after* the passage of the grid. Dye introduced as a vertical line indicated that the jet axes were horizontal and that the velocity profile was approximately symmetric. The jet spacing corresponded to the bar spacing of the grid. Jets behind the horizontal grid bars were in the same direction as the grid motion, while the flow was in the opposite direction in the space between the bars. The jets were more distinct closer to the grid as U/MN decreased, but were never discernible until at least $x \approx 2$ m. Our observations were similar to those of Frenzen (1963). However, Frenzen incorrectly attributed the two-dimensional jets to the blocking effect referred to earlier, but which is not relevant either to Frenzen's or the present results. Well after the passage of the grid, the jet structure died away

leaving a very weak density perturbation on the initially linear profile. The density perturbation was observed with a shadowgraph and appeared as a series of parallel horizontal bands spaced at the mesh size (coincident with the maximum shear in the velocity profile). Attempts to measure this density perturbation with the electronic balance were unsuccessful; the perturbations being too small even at the minimum value of U/NM and the maximum N. When $U/NM \gtrsim 1$ the banded structure was not observed.

3.2. *Plume growth*

In the neutrally stratified grid turbulence both σ_y and σ_z increased steadily with distance downstream from the source. It was interesting to note, though also expected, that the large-scale structure of the plumes, reflected in σ_y and σ_z, was independent of the Reynolds number while our visual observations showed that the fine-scale structure was dependent on the mesh Reynolds number. The lateral growth of the plume in the stable density stratification is not dissimilar to that in the homogeneous fluid; all scales of the flow being little affected. But the growth of σ_z is markedly attenuated by the stable density stratification. The vertical spread of the plume initially increases but then remains approximately constant. Dimensional analysis suggests that the development of the plume width should be expressed as

$$\frac{\sigma_\alpha}{M} = f_\alpha\left(\frac{x_1}{M}, \frac{x}{M}, \frac{U}{NM}\right), \tag{4}$$

where $\alpha = y$ or z for a particular geometry. It is unlikely that molecular effects, viscosity or diffusivity, are relevant provided that the Reynolds and Péclet numbers are large.

If only one source position relative to the grid is considered then

$$\frac{\sigma_\alpha}{M} = f_\alpha\left(\frac{x_1}{M}, \frac{U}{NM}\right), \tag{5}$$

where U/NM has the form of a Froude number. The grouping U/NM is the single non-dimensional parameter describing the influence of the density stratification on the plume growth.

When there is no density stratification $N \to 0$ and $U/NM \to \infty$. The data for this case are shown in figure 2. The results for $U = 6$, 12 and 30 cm/s are similar, confirming the correctness of our omission of a Reynolds number from (4). There is also no significant difference between σ_y and σ_z. For large x_1/M (actually $t \gg T_L$) the data approximate to the curve

$$\frac{\sigma_y, \sigma_z}{M} = 0{\cdot}16\left(\frac{x_1}{M}\right)^{\frac{1}{2}}. \tag{6}$$

This is consistent with a constant diffusion coefficient of $K = 0{\cdot}0128UM$ where $\sigma^2 = 2Kx_1/U$. Alternatively $K = (v'^2, w'^2)\, T_L = \text{const}$, for a non-decaying turbulence. It has been argued by Batchelor (1952) and others that, for decaying grid turbulence, $v'^2 \propto (x - x_0)^{-1}$ and $T_L \propto x - x_0$ over a considerable range of $(x - x_0)/M$, where x_0/M is a virtual origin. Thus, even in decaying grid turbulence the diffusion constant K may be expected to be constant. Thus $T_L = 0{\cdot}0128UM/(v'^2, w'^2)$ for the present experiments. Note that this gives estimates of $UT_L \approx 6{\cdot}5$ cm at $x_1/M = 0$, $x/M = 4{\cdot}71$ and of $UT_L \approx 17{\cdot}0$ cm at $x_1/M = 3{\cdot}53$, $x/M = 8{\cdot}24$. Also included in figure 2 is the anticipated result from the statistical diffusion theory of Taylor (1921) using the average of the standard deviation of velocity fluctuations measured at $x_1/M = 0$ and 3·53.

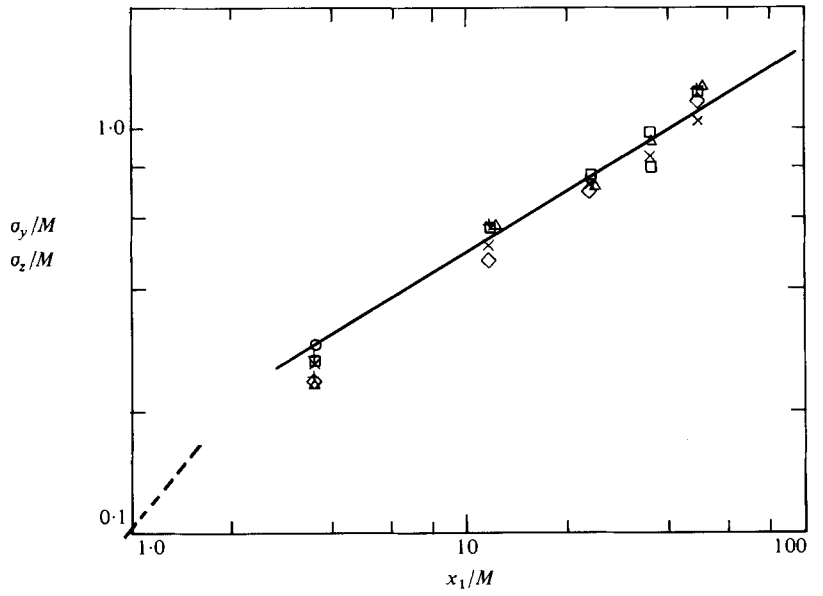

FIGURE 2. The lateral and vertical plume widths in a homogeneous fluid as a function of distance downstream from the source. Horizontal: △, $U = 6$ cm/s; ○, 12 cm/s; ◇, 30 cm/s. Vertical: □, $U = 6$ cm/s; +, 12 cm/s; ×, 30 cm/s. The solid line is equation (6) while the dashed line is the result anticipated at small x_1/UT_L from Taylor (1921). The dye source is at $x/M = 4{\cdot}71$.

The experimental results of plume development when U/NM is finite (figures 3*a*, *b*) show that the horizontal plume width σ_y is not measurably influenced by the density stratification for $U/NM \geqslant 1{\cdot}0$. At values of the Froude number U/NM less than 1·0 there is a 30% reduction in the horizontal plume width at large x_1/M ($\gtrsim 20$). The growth of the plume in the vertical (figure 3*b*) is attenuated by even the smallest density stratification ($U/NM \lesssim 8{\cdot}2$), the attenuation being systematically greater with decreasing U/NM. The best-fit expression (6) for the non-stratified experiments has been included in figures 3(*a*, *b*) for comparison. The growth of each plume's vertical width is characterized by an increase to a maximum and then either a slight decrease to a constant plume width or no decrease and a maintained maximum plume width. It is apparent that the maximum vertical plume width σ_z is a function of the stratification parameter U/NM. In figure 4, $\sigma_{z\infty}$, non-dimensionalized as $\sigma_{z\infty}N/U$ is plotted against U/NM. The data show a systematic decrease as the Froude number increases. A more physically relevant non-dimensionalization might replace the mean velocity with some characteristic turbulent velocity. We choose, somewhat arbitrarily, the root mean square of the velocity fluctuations, w'_{0s}, at the *source position* in a homogeneous fluid. The right-hand ordinate of figure 4 is then $\sigma_{z\infty}N/w'_{0s}$. This parameter is of order unity, varying over the range 1·5–0·5 as U/NM increases from 0·5 to 10.

3.3. *Velocity measurements*

The standard deviation of the velocity fluctuations behind the grid was measured for the cases $N = 0$ and 1·33 rad/s at $U = 12$ cm/s, that is $U/MN = \infty$ and 1·06. The standard deviations normalized with the mean velocity (towing speed) are presented in figures 5(*a*, *b*) as functions of the non-dimensional distance from the grid x/M. The scatter in the more extensive results for the vertical velocity fluctuations is

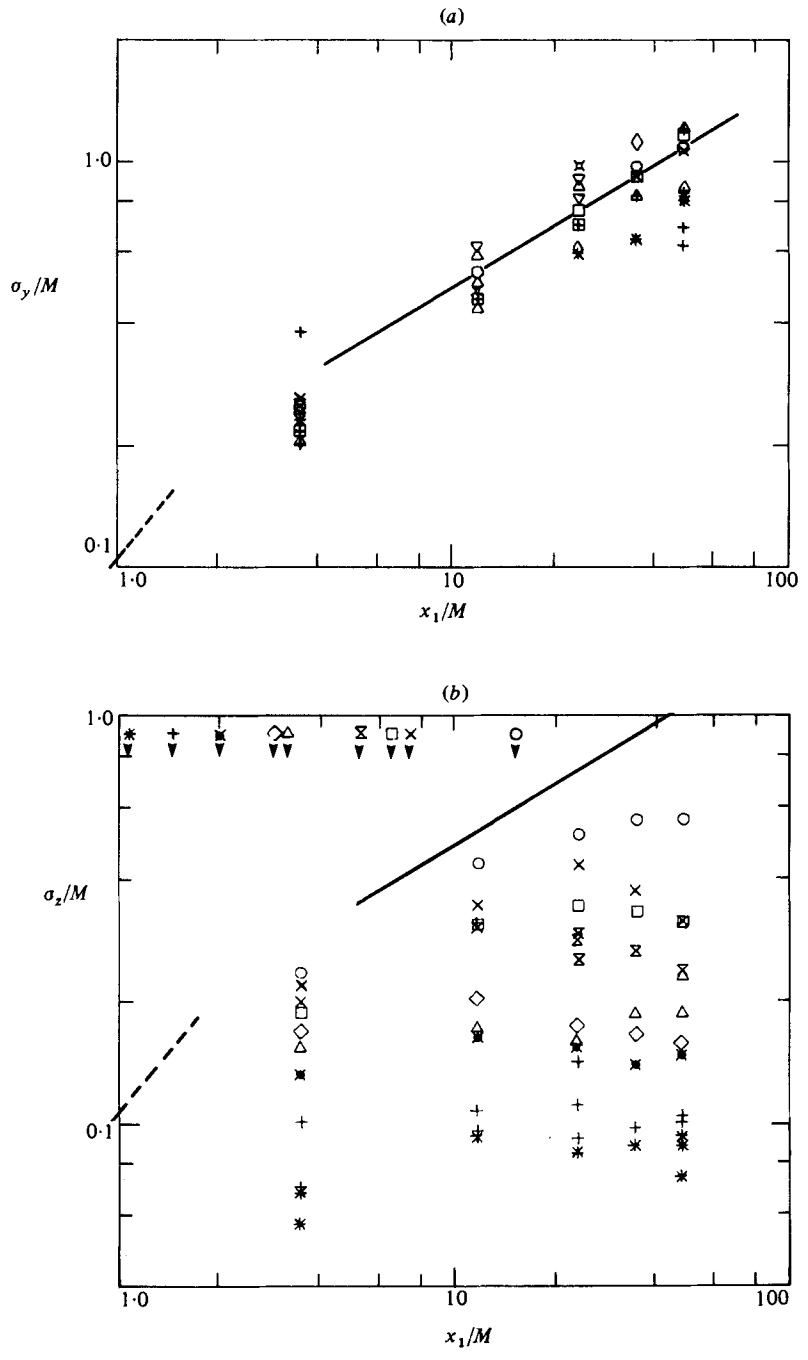

FIGURE 3. The lateral (*a*) and vertical (*b*) plume widths as functions of distance downstream from the source for various Froude numbers U/NM: ○, $U/NM = 8{\cdot}21$; ×, 3·68; □, 3·28; ⧖, 2·65; △, 1·64; ◇, 1·47; ⋈, 1·06; +, 0·735; *, 0·531. The solid and dashed lines are from equation (6) and correspond to $U/NM \to \infty$. The vertical arrows (▼) denote the value of x/M at which $Nt = 2$ for each value of U/NM.

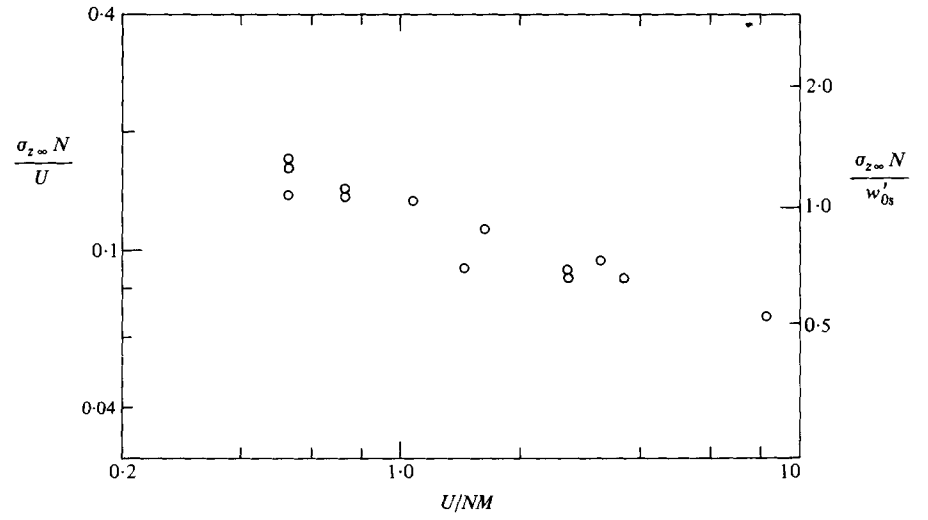

FIGURE 4. The maximum vertical plume width $\sigma_{z\infty}$, non-dimensionalized with (*a*) U/N and (*b*) w'_{0s}/N as a function of the Froude number U/NM.

considerable for the small intensities measured at $x/M > 20$, and this also casts doubt on the accuracy of the lateral velocity fluctuations for $x/M > 20$. Curves of the form

$$\frac{v', w'}{U} = A\left(\frac{x}{M} - B\right)^{-\frac{1}{2}} \tag{7}$$

have been fitted to the data taken with no density stratification with $(A, B) = (0{\cdot}184, 2)$ for the lateral velocity fluctuations and $(0{\cdot}203, 2)$ for the vertical velocity fluctuations. The small difference in velocity fluctuations in the lateral and vertical is unexplained.

Over the range $5 \lesssim x/M \lesssim 50$, $10 \lesssim Nx/U \lesssim 100$ and $w'/NM \gtrsim 0{\cdot}025$ the form of the decay of v'/U and w'/U with x is unchanged by stable stratification from that given in (7). The values of v'/U and w'/U and the two values of the parameter A in (7) were reduced to not less than about 0·9 and 0·7 respectively of their neutral values. Obviously these reductions must be functions of the stratification since they are unity when $U/MN \to \infty$. We find, by plotting v'/U and w'/U at $x/M = 4{\cdot}71$ against U/NM, in figure 6 that $w'/U \propto (U/NM)^{\frac{1}{2}}$ for $0{\cdot}5 \leqslant U/NM \leqslant 5$ and a weaker dependence for v'/U. This result has been determined for only one value of N, though dimensional arguments require only the two dimensionless parameters $(w'/U, U/NM)$.

Measurements of the mean velocity with a propeller anemometer and with the hot-film anemometer indicated that for $N = 0$ the maximum variation in mean velocity behind the grid was less than $\pm 5\%$ for $x/M \geqslant 4{\cdot}71$. Use of the propeller anemometer at $N = 1{\cdot}33$ rad/s and $U = 12$ cm/s indicated no greater non-uniformity of the mean velocity at $x/M = 4{\cdot}71$ and 23·6 than for $N = 0$. However, at $x/M = 47{\cdot}1$ the variation of mean velocity was $\pm 7\%$.

Limited checks were made on the homogeneity of the velocity fluctuations both for $N = 0$ and 1·33 rad/s at $U = 12$ cm/s and for $x/M = 4{\cdot}71$ and 47·1. The velocity fluctuation probe was placed directly downstream of (i) the intersection of two bars, (ii) the midpoint of one bar, and (iii) the centre of the mesh. Variations in the standard deviation of the velocity fluctuations was less than $\pm 5\%$ for any $(U/NM, x/M)$

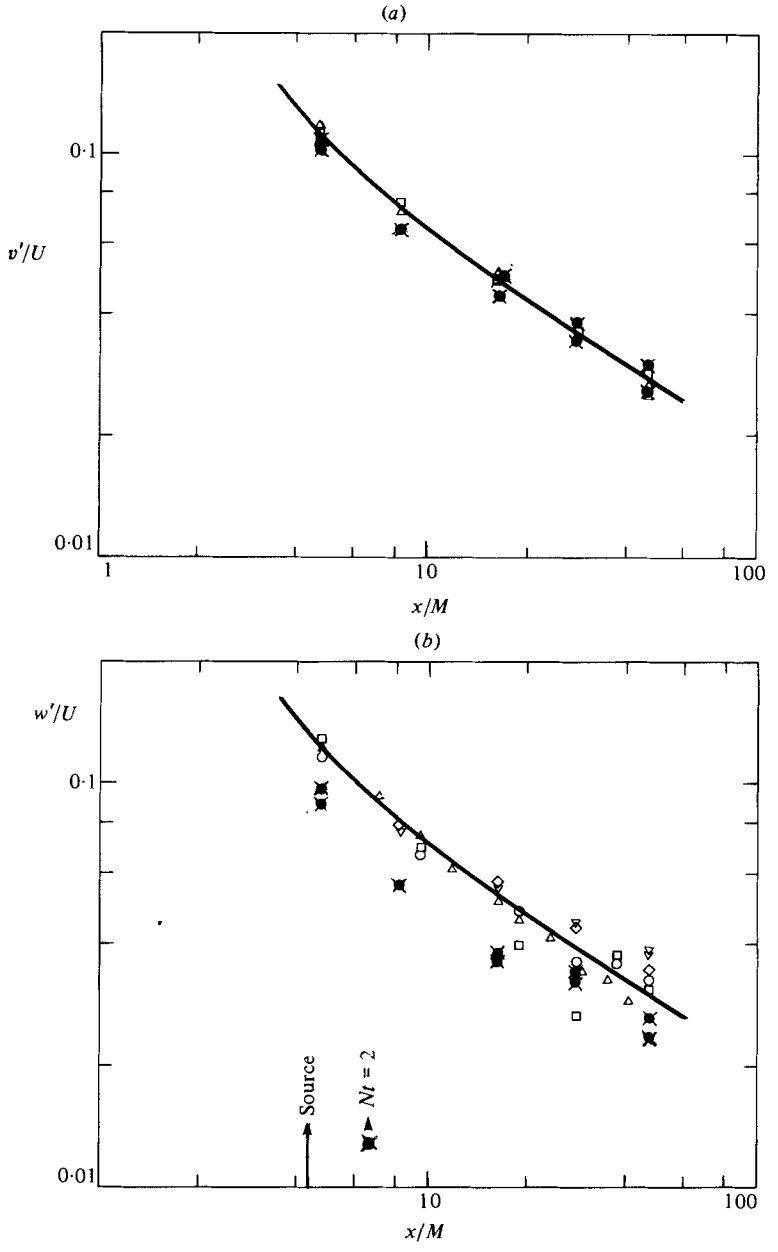

FIGURE 5. Turbulence intensity decay behind the grid. The solid lines are equations (7). (*a*) Lateral v'/U: △, □, $U = 12$ cm/s, $N = 0$; ▣, 12 cm/s, 1·33. (*b*) Vertical w'/U: □, $U = 6$ cm/s, $N = 0$; ▽, ◇, 12 cm/s, 0; △, ○, 30 cm/s, 0; ▣, 12 cm/s, 1·33. The value of x/M at which $Nx/U = Nt = 2$ is indicated by ▲.

combination. Estimates of the jet velocities were made by timing dye traces and with the small propeller anemometer. The jet velocities were very small at $x/M = 4{\cdot}71$ for all $U/MN \geqslant 0{\cdot}532$. The ratios of the jet excess velocity ΔU to the towing speed U increased with x/M to a maximum and then decayed. That is the jets grew out of the 'random' velocity field. This is possibly a result of the biased momentum tagging

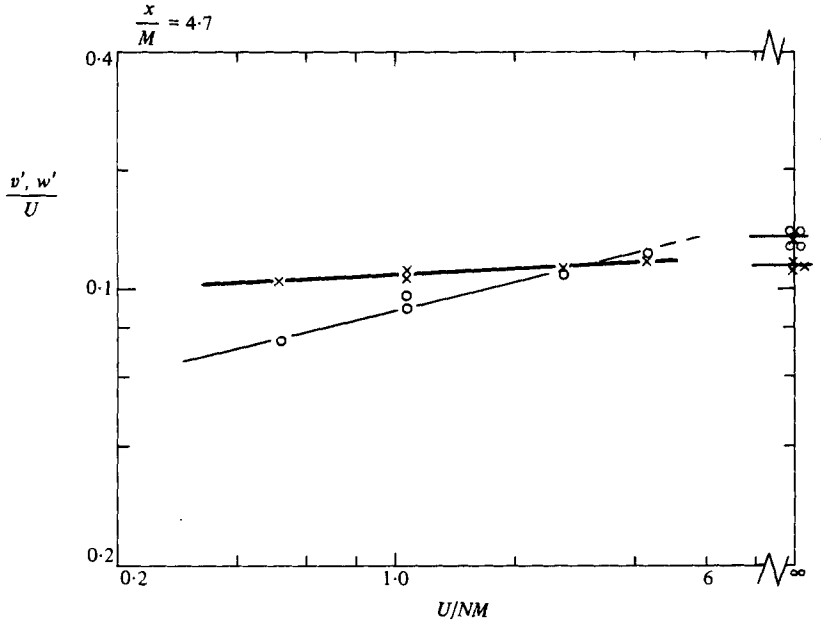

FIGURE 6. Turbulence intensity at the source position as a function of U/NM. ×, v'/U; ○, w'/U.

of particles as they pass through the grid and the subsequent reattainment (for some particles) of their original density level. The ratio of the maximum ΔU to the tow speed appeared to be systematically dependent upon U/NM. This ratio was very small ($< 0{\cdot}03$) at $U/MN = 2{\cdot}65$, approximately 0·1 at $U/MN = 1{\cdot}06$ and 0·15–0·2 at $U/MN = 0{\cdot}532$. The parameter $\Delta U/MN$ was less sensitive to the Froude number and was approximately constant at 0·1.

4. Discussion

4.1. *Decay of turbulence*

First let us consider the implications of our velocity measurements on the general problem of decaying turbulence in a stratified fluid. The results taken in the homogeneous fluid are of the same form as Batchelor & Townsend's (1948) initial-period decay and agree approximately with other measurements (see Comte-Bellot & Corrsin 1966), thus promoting confidence in the measuring system.

The (zero) mean velocity and the turbulence intensity were observed to be uniform across the flow when $x/M \geqslant 4{\cdot}7$ provided that the Froude number was large ($U/NM \gtrsim 2{\cdot}5$). At intermediate values of the Froude number, $1 \lesssim U/NM \lesssim 2{\cdot}5$, the flow remained uniform over the limited range of downstream distances $4{\cdot}7 \leqslant x/M \lesssim 20$. On the other hand, for strongly stratified flows ($U/NM \lesssim 1$) significant non-uniformities were observed at all distances downstream of the grid, and these data should be treated with caution.

Our observation that the decay of the lateral velocity fluctuations are little influenced by density stratification, is consistent with the results of Frenzen (1963), Dickey & Mellor (1980) and Lin & Pao (1979). Frenzen's results were obtained at far weaker stratifications with $U/NM \gtrsim 14$ in a horizontal towing tank similar to but smaller than the one described in the present experiments.

However, these previous experiments show results which were variously different as to the influence of density stratification on the vertical velocity fluctuations. Frenzen (1963) concluded that the vertical velocity fluctuations decayed in the density-stratified fluid in a form similar to that of the decay in the homogeneous fluid. The magnitude of the vertical velocity fluctuations was reduced slightly, less than in the present experiments at the smaller Froude number.

Dickey & Mellor's (1980) experimental results were similar in that the velocity fluctuations initially decayed at about the same rate in the stratified as in the neutral flow, for a certain time t after the grid passed, given by $80 \lesssim Ut/M \lesssim 250$. (In their experiment the grid stopped moving when $Ut/M \approx 50$.) In fact, the r.m.s. vertical velocity (i.e. the component parallel to the grid motion) did not measurably decrease, while the transverse compónents decreased by less than 5 %.

However, when $Ut/M \gtrsim 250$, which was equivalent, at their weak stratification ($U/NM \approx 50$), to $Nt \gtrsim 5$, the vertical velocity fluctuations ceased decaying and the horizontal components decayed at about $\frac{1}{10}$ of the rate in neutral flows. This transition was ascribed by Dickey & Mellor to the sudden appearance of internal waves. On the basis of our discussion in §1.2 we would have expected waves to appear when $2\pi w'/MN \sim 1$. In their experiments waves appeared when $2\pi w'/MN = 1{\cdot}2$ and then the velocity fluctuations decayed very slowly (a well-known feature of internal waves; see Pao 1971). In addition to random waves, there was a *mean* oscillatory motion produced by the grid's motion. This could have been a small extra source of energy for the slowly decaying fluctuations, because, as the wave propagated through the disturbed density gradient, random velocity fluctuations would be generated which would persist as long as the turbulence-induced waves.

By comparison, in our horizontally towed gradient experiment even though w' was small enough for waves to appear ($2\pi w'/MN < 1{\cdot}0$) the r.m.s. velocity fluctuations decayed at a rate almost identical with that in unstratified turbulence. According to the arguments of §1.2, no significant net transfer of wave energy along the tank should have been expected in our experiment, so our decay results can be regarded as local measurements. There was no evidence of any large-scale motions generated by our grid. Presumably internal waves generated at the grid could not propagate downstream because $2\pi U/MN > 1$. In contrast with these results Lin & Pao (1979) using a grid of *vertical* bars towed horizontally, and hot-film anemometers to measure the turbulence, showed that w' decayed more rapidly in stable stratification.

We can conclude from our results and those of Frenzen and Dickey & Mellor that stable stratification does not significantly affect the decay of grid turbulence when $w'/MN > 0{\cdot}1$. Lin & Pao's results are also consistent with this. More precisely, it does not change (to within the errors of this experiment) the ratio of kinetic energies at two downstream planes x_2, x_3 (or at two times after the passage of the grid) i.e. $\overline{q^2}(x_2/M)/\overline{q^2}(x_3/M)$. However, there is a small *reduction* by about 16 % in the dissipation rate normalized on the local velocity fluctuations and grid scale. This *could* be caused by about a 16 % reduction in the integral scale. (It is interesting to recall Dougherty's (1961) and Brost & Wyngaard's (1978) suggestions that in atmospheric turbulence the scale of turbulence cannot be greater than about $2\pi w'/N$ in stable conditions. This is probably correct; however, this scale does not appear to be a generally applicable integral scale relevant for estimating dissipation. If it was, the dissipation rate in an experiment would have increased by about a factor of 3 in the strongest stratification.)

When $w'/MN \approx 0{\cdot}15$ Dickey & Mellor observe internal waves and a reduced decay rate; we do not observe these even at $w'/MN \approx 0{\cdot}03$ while Lin & Pao indicate an increased decay rate for $w'/MN < 0{\cdot}03$.

The cause of the different observations is still not clear, though the initial conditions are noted to be different for each experiment.

4.2. *Diffusion experiments*

A naive inspection of the measurements for the decay of v' and w' with and without stable stratification might suggest that σ_y and σ_z should also be largely unaffected. However, the results show that, although this prediction is true for σ_y when $1 \lesssim U/MN \lesssim \infty$, it is not true for any measurement of σ_z over the observed range of U/NM ($< 8{\cdot}2$).

The reduction and levelling off of σ_z with distance from the source as U/NM decreases might at first be attributed to:

(i) the velocity fluctuations w' decaying more rapidly;

(ii) the velocity fluctuations consisting mainly of internal waves;

(iii) a selective damping of the largest spatial scales of turbulence.

Our own data shows that the first of these is not true, while Frenzen's and Dickey & Mellor's measurements of correlation functions show that the latter two points are not true either in weakly stratified grid turbulence. In our most strongly stratified cases internal waves and selective damping of scales probably occurs, but the flow is still turbulent and decaying at the same rate as in neutral flow.

As we have described briefly in §1.2, Csanady (1964) and Pearson *et al.* (1983) have put forward a theoretical model for particle motions. They show that particles do not have sufficient kinetic energy to move vertically more than a distance of $O(w'/N)$, provided that the timescale k_{D}^{-1} for particles to change their density is long compared with N. (The spatial scales over which velocities are correlated may be significantly greater than $O(w'/N)$.)

To compare the predictions of Pearson *et al.* (1982), the results should ideally be plotted in terms of the asymptotic growth of the plume $\sigma_{z\infty} N/w'_{\mathrm{s}} = f(T_{\mathrm{L}} N)$, where T_{L} is a Lagrangian timescale of the turbulence.

However, to compare the present experimental results with the analysis above we form the dependent variable $\sigma_{z\infty} N/w'_{\mathrm{s}}$, where w'_{s} is the standard deviation of the vertical velocity fluctuations at the source, and plot it against the independent variable U/NM. The ratio M/U has roughly the same magnitude as the time constant T_{L} (Snyder & Lumley 1971). A plot of $\sigma_{z\infty} N/w'_{\mathrm{s}}$ against the Froude number U/NM (figure 7) does show the anticipated decrease with U/NM, and also indicates that $\sigma_{z\infty} N/w'_{\mathrm{s}}$ varies in the range 0·5–2·0, quite close to the estimates given by both Csanady (1964) and by Pearson *et al.* (1982). Pearson *et al.* (1982) also predict that the plume reaches about 75 % of the final vertical width $\sigma_{z\infty}$ when $1 < Nt < 2$, where $t = x_1/U$. Our results show that, within the range of parameters considered, the influence of stratification is felt when $Nt \sim 1$, and the plume reaches its maximum width when $Nt \simeq 2$, as may be seen in figure 3(*b*), where we indicate the value of x_1/M at which $Nt = 2$.

To emphasize the key point again, these experiments show that for the turbulent diffusion of dye (in a salt-water solution) in stably stratified homogeneous grid turbulence $d\sigma_z^2/dt$ is zero (to within experimental error) when $Nt \gtrsim 3$. This is inconsistent with a finite value of K_z when the plume has levelled out. There are still velocity fluctuations at this stage and they are decaying at about the same rate as neutral turbulence. There is no evidence that these fluctuations are simply internal waves.

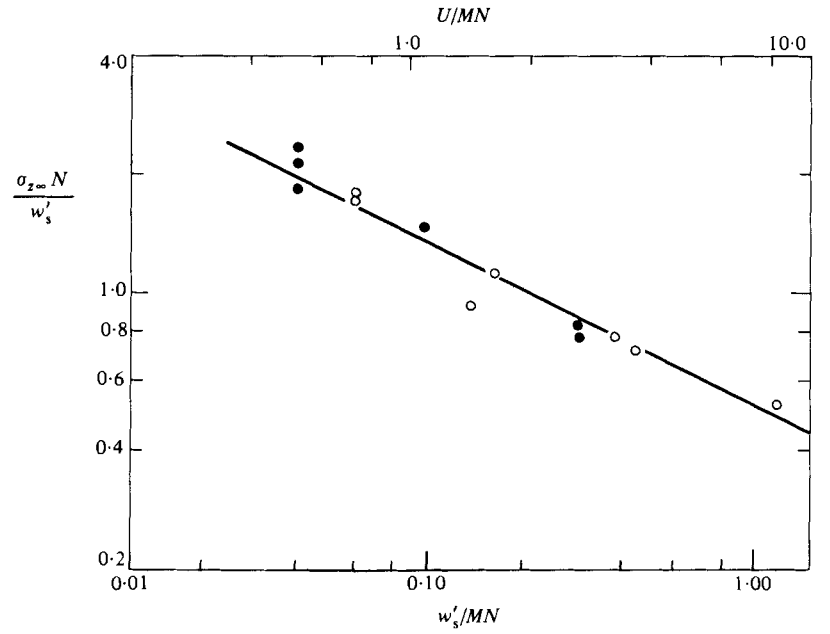

FIGURE 7. The variation of $\sigma_{z\infty} N/w_s'$ with U/NM. The solid symbols are based on an interpolation from figure 6.

4.3. *Application to other fluids and flows*

These diffusion results are not directly comparable with diffusion measurements from point sources in the stable atmospheric boundary layer, where variations of the mean velocity and turbulence scale may be significant over the plume depth. However, it is worth noting that the form of lateral horizontal diffusion from point sources is very similar in stable and in neutral conditions. Secondly, limited vertical diffusion from *elevated* sources is quite often observed; a few cases are discussed in detail by Pearson *et al.* (1983), and the differences between diffusion from ground level and elevated sources is discussed by Hunt (1982).

Finally, a cautionary point needs to be made about the general application of these results to other stratified turbulent flows. We have discussed in §1.2 how the energy production and dissipation in such flows may be more or less local in its origin depending on orientation of the flow and the geometry of bounding surfaces. More research on this question is clearly necessary.

It is also important to realize that the role of the molecular diffusion of matter is more important in very stable conditions when the vertical motion of fluid elements is constrained. For reasons given by Pearson *et al.* (1983), significantly different results may be expected if the diffusivity ν_C of the contaminant (dye in this case) is markedly different to the diffusivity ν_D of the density of fluid elements (salt in this case). In this case (dye and salt) $\nu_C \sim \nu_D$; but in the case of smoke particles in the atmosphere $\nu_C \ll \nu_D$.

R.E.B. and J.C.R.H. gratefully acknowledge financial support provided through appointments at North Carolina State University under U.S. Environmental Protection Agency Grant 805595. The authors are grateful for referees' helpful comments.

REFERENCES

ARMI, L. 1978 Some evidence for boundary mixing in the deep ocean. *J. Geophys. Res.* **83**, 1971–1979.

BATCHELOR, G. K. 1952 Diffusion in a field of homogeneous turbulence. II. The relative motion of particles. *Proc. Camb. Phil. Soc.* **48**, 345–362.

BATCHELOR, G. K. & TOWNSEND, A. A. 1948 Decay of isotropic turbulence in the initial period. *Proc. R. Soc. Lond.* **A193**, 539–566.

BRITTER, R. E. & MARSH, G. L. 1982 Potential energy changes in a transient experiment on density stratified turbulence (in preparation).

BROST, R. A. & WYNGAARD, J. C. 1978 A model study of the stably stratified planetary boundary layer. *J. Atmos. Sci.* **35**, 14–28.

COMTE-BELLOT, G. & CORRSIN, S. 1966 The use of a contraction to improve the isotropy of grid-generated turbulence. *J. Fluid Mech.* **24**, 657–682.

CSANADY, G. 1964 Turbulent diffusion in a stratified fluid. *Atmos. Sci.* **21**, 439–447.

DICKEY, T. D. & MELLOR, G. L. 1980 Decaying turbulence in neutral and stratified fluids. *J. Fluid Mech.* **99**, 13–32.

DOUGHERTY, J. P. 1961 The anisotropy of turbulence at the meteor level. *J. Atmos. Terr. Phys.* **21**, 210–213.

FRENZEN, P. 1963 A laboratory investigation of the Lagrangian autocorrelation function in a stratified fluid. *Argonne National Lab. Rep.* ANL-6794.

HUNT, J. C. R. 1982 Diffusion in the stable boundary layer. In *Atmospheric Turbulence and Air Pollution Modelling* (ed. F. T. M. Nieuwstadt & H. Van Dop), pp. 231–274. Reidel.

HUNT, J. C. R. & SNYDER, W. H. 1980 Experiments on stably and neutrally stratified flow over a model three-dimensional hill. *J. Fluid Mech.* **96**, 671–704.

IBBETSON, A. & TRITTON, D. J. 1975 Experiments on turbulence in a rotating fluid. *J. Fluid Mech.* **68**, 639–672.

KAIMAL, J. C. 1973 Turbulence spectra, length scales and structure parameters in the stable surface layer. *Boundary-Layer Met.* **4**, 289–309.

LIN, J. T. & PAO, Y. H. 1979 Wakes in stratified fluids. *Ann. Rev. Fluid Mech.* **11**, 317–338.

LINDEN, P. F. 1980 Mixing across a density interface produced by grid turbulence. *J. Fluid Mech.* **100**, 691–703.

MCLAREN, T. I., PIERCE, A. D., FOHL, T. & MURPHY, B. C. 1973 An investigation of internal gravity waves generated by a buoyancy rising fluid in a stratified medium. *J. Fluid Mech.* **57**, 229–240.

PAO, Y. H. 1971 Turbulence measurements in stably stratified fluids. In *Turbulence Measurements in Liquids*. Dept of Chemical Engineering, University of Missouri–Rolla.

PASQUILL, F. 1974 *Atmospheric Diffusion*, 2nd edn. Ellis Harwood.

PEARSON, H. J. & BRITTER, R. E. 1980 A statistical model for vertical turbulent diffusion in stably stratified flow. In *Proc. 2nd I.A.H.R. Symp. on Stratified Flows, Trondheim, Norway*, (ed. T. Carstons & T. McClimans), pp. 269–279. Tapir.

PEARSON, H. J., PUTTOCK, J. S. & HUNT, J. C. R. 1983 A statistical model of fluid element motions and vertical diffusion in a homogeneous stratified flow. *J. Fluid Mech.* (to be published).

SNYDER, W. H. & LUMLEY, J. 1971 Some measurements of particle velocity autocorrelation functions in a turbulent flow. *J. Fluid Mech.* **48**, 41–71.

TAYLOR, G. I. 1921 Diffusion by continuous movements. *Proc. Lond. Math. Soc.* (*Ser.* 2) **20**, 196–212.

TURNER, J. S. 1973 *Buoyancy Effects in Fluids*. Cambridge University Press.

WEINSTOCK, J. 1978 Vertical turbulent diffusion in a stably stratified fluid. *J. Atmos. Sci.* **35**, 1022–1027.